Surface passivation of crystalline silicon by Cat-CVD amorphous and nanocrystalline thin silicon films

C.Voz[1], I. Martin[1], A. Orpella[1], J. Puigdollers[1], M. Vetter[1] and R. Alcubilla[1]

D. Soler[2], M. Fonrodona[2], J. Bertomeu[2] and J. Andreu[2]

[1] Departament d'Enginyeria Electronica, Universitat Politecnica de Catalunya, Gran Capita s/n, Modul C4, Barcelona 08034, Spain

[2] Departament de Fisica Aplicada i Optica, Universitat de Barcelona, Av. Diagonal 647, Barcelona 08028, Spain

Abstract

In this work we study the electronic surface passivation of crystalline silicon with intrinsic thin silicon films deposited by Catalytic CVD. The contactless method used to determine the effective surface recombination velocity was the Quasi-Steady-State Photoconductance technique. Hydrogenated amorphous and nanocrystalline silicon films were evaluated as passivating layers on n- and p-type float zone silicon wafers. The best results were obtained with amorphous silicon films which allowed effective surface recombination velocities as low as 60 and 130 cm s^{-1} on p- and n-type silicon respectively. To our knowledge, these are the best results ever reported with intrinsic amorphous silicon films deposited by Catalytic CVD. The passivating properties of nanocrystalline silicon films strongly depend on the deposition conditions, specially on the filament temperature. Samples grown at lower filament temperatures (1600 ºC) allowed effective surface recombination velocities of 450 and 600 cm s^{-1} on n- and p-type silicon.

Keywords

Passivation, Catalytic CVD, Heterostructures, Solar cells

1. Introduction

As manufacturers of crystalline silicon (c-Si) solar cells use thinner wafers to reduce costs, electronic surface passivation becomes very important to the achievement of high efficiencies. The classical method for the passivation of silicon wafers is the thermal oxidation at high temperature (> 1000º C). Nevertheless, the high temperatures used during the thermal oxide growth not only degrade the bulk carrier lifetime but are also undesirable from production cost and throughput considerations. Hence, significant effort has been devoted to the development of alternative low temperature (< 500 ºC) surface passivation alternatives. One of the most successful approaches has been the use of silicon nitride layers (SiN_x) [1] deposited by plasma enhanced chemical vapour deposition (PECVD). More recently, heterojunctions using amorphous silicon carbide layers deposited by PECVD evidenced excellent passivation properties [2]. Since these thin silicon films can be doped during the deposition process, they open the possibility to obtain low temperature heterojunction solar cells like the so-called HIT (Heterojunction with Intrinsic Thin layer) structure [3]. However, very few results concerning the use of Cat-CVD for passivating c-Si surfaces have been reported to date. Van Cleef et al. reported an effective surface recombination velocity of 84 cm s^{-1} with intrinsic a-Si:H films on p-type c-Si [4]. An annealing step at 300 ºC for 30 minutes was required to achieve this value. There are several reasons justifying why the Cat-CVD technique could be suitable for passivation purposes: (a) the high concentration of atomic hydrogen in the chamber during Cat-CVD processes could passivate the dangling bonds at the c-Si surface, and (b), the absence of ion bombardment could result beneficial to reduce the density of traps at the interface [5]. In this

work we study the electronic passivation of c-Si surfaces by Cat-CVD amorphous and nanocrystalline thin silicon films.

2. Experimental

All the samples in this work were obtained by Cat-CVD in an ultra-high vacuum (UHV) deposition system described elsewhere [6]. The dissociation of the gases was achieved by means of a tantalum wire 0.5 mm in diameter. The basket-shaped wire, with three loops near the gas inlet, allows a high dissociation of the incoming gas flows. The distance between the upper part of the wire and the substrate holder was 3 cm. The radiation of the wire at usual process temperatures (1500-1800 ºC) heats the substrate to 150 ºC. Additional heating up to 300 ºC is achieved by means of a heater attached to the substrate holder. The hydrogen content of the films was measured by Fourier Transform Infrared (FTIR) spectrometry and the optical absorption coefficient by Photothermal Deflection Spectroscopy (PDS). Float Zone (FZ) silicon wafers (100) with long bulk lifetimes (τ_B >1 ms) were used for the passivation studies. The resisitivities of p- and n-type wafers were 3.3 Ω cm and 1.4 Ω cm respectively, which are near the doping levels used by the photovoltaic industry. Before deposition, the silicon wafers were cleaned in a H_2SO_4:H_2O_2 (2:1) solution, dipped in 5% HF and immediately introduced into the UHV system. The effective lifetime (τ_{eff}) as a function of the excess minority carrier density was measured by the contactless Quasi-Steady-State Photoconductance technique (QSS-PC) using the instrument Sinton WCT-100 [7]. Additionally, an hydrogen Cat-CVD treatment was also tested as an alternative to the wet cleaning procedure. It consisted in exposing the c-Si surface to 20 sccm of hydrogen dissociated by the wire heated to 1700 ºC. Thereby, the native silicon oxide is etched by the atomic hydrogen for 10 minutes at a process pressure of 3×10^{-2} mbar. In table 1 we show the deposition parameters of the Cat-CVD thin silicon films studied in this work: hydrogenated nanocrystalline silicon (nc-Si:H) films grown at low (L) and high (H) filament temperatures, and an optimised hydrogenated amorphous silicon (a-Si:H) film. The thicknesses of the samples on

c-Si for electronic passivation studies were around 200 nm, whereas films over 1 μm thick were deposited for other characterisations.

3. Results

An extensive structural characterisation of thin silicon films grown under the same deposition conditions in table 1 has been previously reported [8]. Considering the nc-Si:H films, the X-ray diffraction spectra show that the crystalline preferential orientation changes from (220) to (111) when the filament temperature is increased. Nevertheless, the crystalline fraction determined by Raman spectroscopy was over 95% regardless of the filament temperature. In figure 1 we show the FTIR spectra used for the calculation of the hydrogen content in the films. The a-Si:H presented the highest hydrogen content of 11%, whereas the nc-Si:H(L) sample had double hydrogen content (7%) than the nc-Si:H(H) one (3%). All the samples presented a low subgap optical absorption measured by PDS, which points to defect densities below 10^{16} cm^{-3}. For electronic passivation studies, each thin silicon film in table 1 was tested on p- and n-type c-Si wafers. The effective lifetimes in figure 2 were measured by the QSS-PC technique over four orders of magnitude of the excess minority carrier density. The values corresponding at an excess minority carrier density of 10^{15} cm^{-3} (≈1 sun illumination) are given in table 2. The effective surface recombination velocity (S_{eff}) is calculated according to $S_{eff}=W / 2\tau_{eff}$ [9] where W is the wafer thickness (350 μm).

The nc-Si:H films grown at the lower filament temperature (1600 ºC) resulted in higher τ_{eff} values than those grown at the higher filament temperature (1800 ºC). Besides, the electronic passivation was slightly better on n-type silicon wafers. Nevertheless, the best results were obtained for the optimised a-Si:H film, which yielded minimum S_{eff} values on p- and n-type wafers of about 60 and 130 cm s^{-1} respectively. These values were obtained without any annealing step and remained stable under light soaking for several weeks. As an additional experiment, a-Si:H films were also grown on wafers cleaned by the Cat-CVD hydrogen

treatment described in section 2. Although minimum S_{eff} values of about 90 cm s^{-1} were achieved on p-type wafers, much poorer results were obtained on n-type silicon (800 cm s^{-1}). For that reason, the Cat-CVD hydrogen treatment was discarded as a suitable cleaning procedure.

4. Discussion

In order to get a further insight into the QSS-PC data, we fitted the results according to a model widely described in a previous work [10]. Within this model we consider field-effect passivation due to a strong band bending (inversion) in the c-Si surface. The parameters to determine within the model are the fixed charge density at the interface (Q_f) and the fundamental surface recombination velocities for electrons (S_n) and holes (S_p). On the one hand, Q_f depends on the defect density (N_d) and the width of the depletion region (w) in the thin silicon film ($Q_f = N_d\, w$). On the other hand, S_n and S_p are defined as $S_{n/p}=v_{th}\sigma_{n/p}D_{it}$ where v_{th} is the thermal velocity, $\sigma_{n/p}$ are the capture cross section of electron/holes by the recombination centers and D_{it} the interface density of states at midgap. The values in table 3 allowed to simulate the QSS-PC data in figure 2 over three orders of magnitude of the excess minority carrier density. Considering that in any case the defect density of the thin silicon films is below 10^{16} cm^{-3}, the fixed charge density in the order of 10^{11} cm^{-2} points to a depletion region width over 100 nm. The change in the sign of Q_f from n- to p-type wafers can be attributed to the amphoteric character of the dangling bonds. The band bending in the thin silicon film forces the dangling bonds to be positively or negatively charged on p- and n-type wafers respectively. Furthermore, in n-type wafers the recombination velocity of holes is higher than for electrons because the interface recombination centers are negatively charged. The opposite occurs on p-type wafers where they are positively charged. Since the model evidences only slight differences in Q_f, the passivating properties correlate with the surface recombination velocities. Considering that the interface recombination centers are dangling bonds, the capture cross sections should not vary between the samples. Note that in table 3 the S_n / S_p ratio remains invariable for all the samples on the same doping type wafer.

Therefore, the differences could be attributed to variations in D_{it}. The higher hydrogen content of the a-Si:H (11%) could be responsible for the longer τ_{eff} by passivating interface recombination centers. In the case of the nc-Si:H films, apart from the hydrogen content, the different crystalline preferential orientations could also have an influence. The density of silicon bonds at the interface of a (111) plane is a factor 1.6 higher than for a (220) one. This could lead to a higher density of interface recombination centers.

5. Conclusions

The electronic passivation of both n- and p-type c-Si surfaces by Cat-CVD thin silicon films has been studied. The best results were obtained with a-Si:H films which allowed S_{eff} values as low as 60 and 130 cm s^{-1} on p- and n-type c-Si respectively. These values were achieved without any annealing treatment and remained stable under light soaking for several weeks. The use of nc-Si:H films deposited at low filament temperatures still allowed S_{eff} values of 450 and 600 cm s^{-1} on n- and p-type c-Si. Future work will concentrate on the incorporation of doped thin silicon films to fabricate heterojunction solar cells fully processed at low temperatures.

Acknowledgements

This research was supported by the CICYT of the Spanish Government under programme MAT2001-3541-C03 (APSIDE).

References

1. T. Lauinger, J. Schmidt, A.G. Aberle, R. Hezel, Appl. Phys. Lett. 68 (1996) 1232.
2. I. Martin, M. Vetter, A. Orpella, J. Puigdollers, A. Cuevas, R. Alcubilla, Appl. Phys. Lett. 79 (2001) 2199.

3. M. Taguchi, K. Kawamoto, S. Tsuge, T. Baba, H. Sakata, M. Morizane, K. Uchihashi, N. Nakamura, S. Kiyama, O. Oota, Prog. Photovolt.: Res. Appl. 8 (2000) 503.
4. M.W.M. Van Cleef, F.M. Schuurmans, A.S.H. Van der Heide, A. Schönecker, R.E.I. Schropp, Proceedings of the 2nd World Conference on Photovoltaic Solar Energy Conversion, Vienna, Austria, July 6-10, 1998, p. 1661.
5. F. Jansen, I. Chen, M.A. Machonkin, J. Appl. Phys. 66 (1989) 5749.
6. C. Voz, D. Peiro, J. Bertomeu, D. Soler, M. Fonrodona, J. Andreu, Mater. Sci. Eng. B 69/79 (2000) 278.
7. R.A. Sinton, A. Cuevas, Appl. Phys. Lett. 69 (1996) 2510.
8. M. Fonrodona, D. Soler, J.M. Asensi, J. Bertomeu, J. Andreu, J. Non-Cryst. Solids 299-302 (2002) 14.
9. F.M. Schuurmans, A. Schoenecker, A.R. Burgers, W.C. Sinke, Appl. Phys. Lett. 71 (1997) 1795.
10. I. Martin, M. Vetter, A. Orpella, J. Puigdollers, C. Voz, L.F. Marsal, J. Pallares, R. Alcubilla, Thin Solid Films 403-402 (2002) 476.

List of table and figure captions

Table 1. Deposition conditions of the Cat-CVD thin silicon films. The substrate temperature was 300 ºC for all the samples.

Figure 1. Si-H wagging band of the FTIR spectra for the samples in table 1. The hydrogen content of the nc-Si:H samples decreases from 7 to 3% with the filament temperature. It was 11% in the a-Si:H film.

Figure 2. Effective lifetime determined by the QSS-PC technique for the different thin silicon films in table 1 on p-type (a) and n-type (b) FZ silicon wafers. The simulations are discussed in the section 3.

Table 2. Effective lifetime and surface recombination velocity measured by the QSS-PC technique at an excess minority carrier density of 10^{15} cm^{-3}.

Table 3. Parameters used for the simulations in figure 2. S_n and S_p are the fundamental surface recombination velocities of electrons and holes and Q_f is the fixed charge at the thin silicon film.

Table 1

sample	P (mbar)	T_f (ºC)	SiH_4 (sccm)	H_2 (sccm)	r_d (Å s^{-1})
nc-Si:H(L)	3×10^{-2}	1600	4	76	2.5
nc-Si:H(H)	3×10^{-2}	1800	4	76	3.3
a-Si:H	10^{-2}	1700	4	-	1.7

Table 2

sample	wafer	τ_{eff} (μs)	S_{eff} (cm s^{-1})
nc-Si:H(L)	n	40	450
	p	30	600
nc-Si:H(H)	n	20	900
	p	20	900
a-Si:H	n	140	130
	p	300	60

Table 3

sample	wafer	S_n (cm s^{-1}) $\times 10^3$	S_p (cm s^{-1}) $\times 10^3$	Q_f (cm^{-2}) $\times 10^{11}$
nc-Si:H(L)	n	3.0	90	-1.2
	p	320	3.8	+1.2
nc-Si:H(H)	n	7.0	210	-1.1
	p	400	4.8	+1.1
a-Si:H	n	0.77	23	-1.0
	p	20	0.24	+1.0

Figure 1

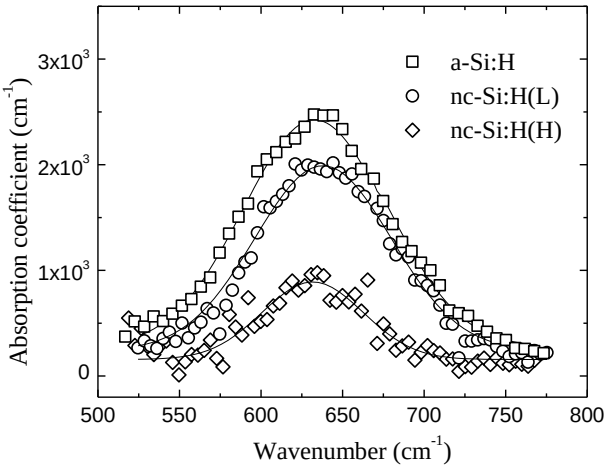
3x10^3
2x10^3
1x10^3
0
Absorption coefficient (cm^-1)
500
550
600
650
700
750
800
Wavenumber (cm^-1)
a-Si:H
nc-Si:H(L)
nc-Si:H(H)

Figure 2

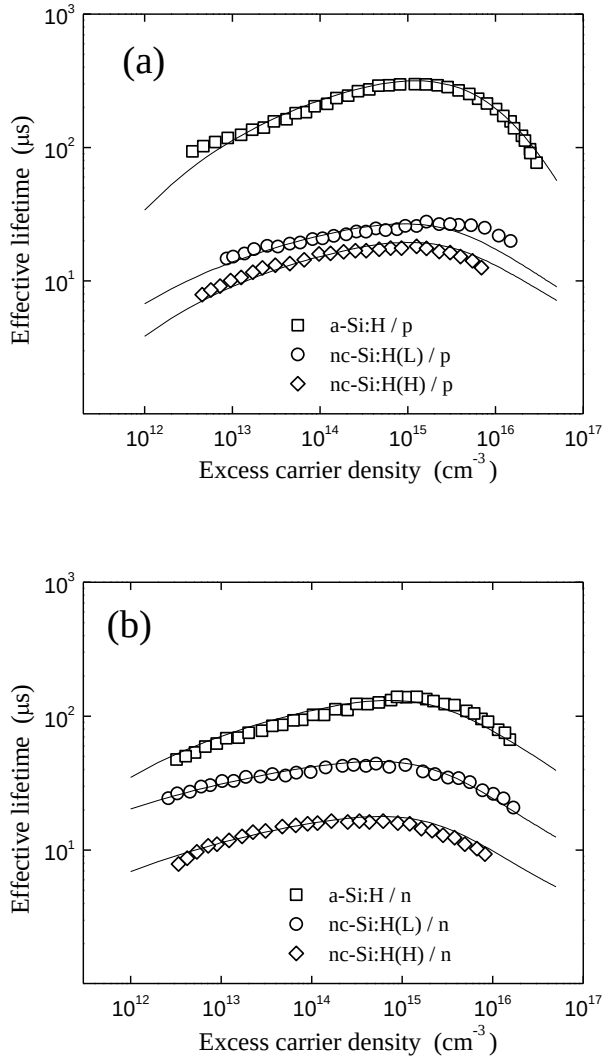
(a)
Effective lifetime (μs)
Excess carrier density (cm-3)
a-Si:H / p
nc-Si:H(L) / p
nc-Si:H(H) / p
(b)
Effective lifetime (μs)
Excess carrier density (cm-3)
a-Si:H / n
nc-Si:H(L) / n
nc-Si:H(H) / n